

Structure and interface chemistry of perovskite-spinel nanocomposite thin films

Cite as: Appl. Phys. Lett. **89**, 172902 (2006); <https://doi.org/10.1063/1.2364692>

Submitted: 14 February 2006 . Accepted: 07 September 2006 . Published Online: 25 October 2006

Q. Zhan, R. Yu, S. P. Crane, H. Zheng, C. Kisielowski, and R. Ramesh



View Online



Export Citation

ARTICLES YOU MAY BE INTERESTED IN

Multiferroic magnetoelectric composites: Historical perspective, status, and future directions
Journal of Applied Physics **103**, 031101 (2008); <https://doi.org/10.1063/1.2836410>

Deposition of epitaxial BiFeO₃/CoFe₂O₄ nanocomposites on (001) SrTiO₃ by combinatorial pulsed laser deposition

Applied Physics Letters **100**, 092901 (2012); <https://doi.org/10.1063/1.3690957>

Three-dimensional heteroepitaxy in self-assembled BaTiO₃-CoFe₂O₄ nanostructures

Applied Physics Letters **85**, 2035 (2004); <https://doi.org/10.1063/1.1786653>



Your Qubits. Measured.

Meet the next generation of quantum analyzers

- Readout for up to 64 qubits
- Operation at up to 8.5 GHz, mixer-calibration-free
- Signal optimization with minimal latency

Find out more



Structure and interface chemistry of perovskite-spinel nanocomposite thin films

Q. Zhan^{a)}

Department of Materials Science and Engineering, University of California, Berkeley, California 94720 and Department of Physics, University of California, Berkeley, California 94720

R. Yu

Materials Sciences Division, Lawrence Berkeley National Laboratory, Berkeley, California 94720

S. P. Crane and H. Zheng

Department of Materials Science and Engineering, University of California, Berkeley, California 94720 and Department of Physics, University of California, Berkeley, California 94720

C. Kisielowski

National Center for Electron Microscopy, Materials Sciences Division, Lawrence Berkeley National Laboratory, Berkeley, California 94720

R. Ramesh

Department of Materials Science and Engineering, University of California, Berkeley, California 94720 and Department of Physics, University of California, Berkeley, California 94720

(Received 14 February 2006; accepted 7 September 2006; published online 25 October 2006)

The structure and the interface chemistry of epitaxial $\text{BiFeO}_3\text{-NiFe}_2\text{O}_4$ nanocomposite thin films on $\text{SrTiO}_3(001)$ substrates were investigated using the Z-contrast imaging and the electron exit-wave reconstruction methods at the atomic scale. The results show that the NiFe_2O_4 pillars are nonwetting with respect to the substrate and exhibit $\{111\}$ facets at the surface. The interface between BiFeO_3 and NiFe_2O_4 lies in the $\{110\}$ planes and is semicoherent. The atomic configuration of the interface, with the BiFeO layer bonding to the $[\text{Ni,Fe}]\text{O}_2$ layer, was shown to have the maximized structure continuity and minimized interface charging. © 2006 American Institute of Physics.

[DOI: 10.1063/1.2364692]

Epitaxial nanostructured composite thin films usually show unique properties that are not present in the corresponding single-phase materials.¹⁻³ For example, the structure and magnetoresistance of perovskite manganites can be tuned by the tensile stress originating from the epitaxial secondary phase MgO .¹ Also, self-assembled nanocomposite magnetoelectric thin films have been developed by combining two kinds of oxide phases: one a ferroelectric perovskite and the other a ferrimagnetic spinel.² The composite thin films show a strong magnetoelectric coupling between the two phases.^{2,4} Our studies so far have demonstrated that such self-assembled nanostructures can be formed from many perovskite-spinel combinations.

The enhancement in the properties of nanocomposite thin films results primarily from the interaction between the component phases. An important means to control such interaction is tuning the self-assembly patterns. Recently we showed that different patterned nanostructures can be realized simply by selecting single crystal substrates with different orientations.⁵ Another critical issue controlling the interaction is the interface between the component phases. The chemistry and structure of the interface are a prerequisite to understand the coupling mechanism among ferroelectricity, magnetism, and elasticity. The perovskite-spinel interface is also of great interest in complex oxide-based magnetic tunnel junctions,⁶ since studies have illustrated the importance of the electrode/barrier interface to obtain large junction magnetoresistance.

In this letter, the structures of the epitaxial nanostructured thin films formed by perovskite and spinel have been investigated at the nano and atomic scales using advanced transmission electron microscopy (TEM) techniques. We focus on the heteroepitaxial composite thin film formed by perovskite BiFeO_3 and spinel NiFe_2O_4 . We are using this and the related $\text{BiFeO}_3\text{-CoFe}_2\text{O}_4$ systems as model systems. BiFeO_3 (BFO) is emerging as an attractive ferroelectric material due to its large ferroelectric polarization.⁷ It has a rhombohedrally distorted perovskite structure.⁸ NiFe_2O_4 (NFO) and CoFe_2O_4 (CFO) are ferrimagnetic materials with the spinel structure.⁹ In spinel crystallography, they are written as $(\text{Fe})[\text{Ni,Fe}]_2\text{O}_4$ and $(\text{Fe})[\text{Co,Fe}]_2\text{O}_4$, where the parentheses refer to ions in tetrahedral and the brackets to ions in octahedral sites.

The nanocomposite thin films were grown from targets with different volume fractions of the component phases by pulsed laser deposition (PLD) at 700 °C on $(001)\text{-SrTiO}_3$ (STO) single crystal substrates, upon which an ~ 60 nm thick SrRuO_3 (SRO) bottom electrode was grown by PLD. Details of the deposition procedure are reported elsewhere.¹⁰ Cross-section as well as plan-view samples for TEM studies were prepared by standard ion milling techniques. Structural investigations have been carried out using a Philips CM300 with a point to point resolution of 1.7 Å and information resolution of 0.8 Å and an FEI Tecnai F20 equipped with high-angle annular dark-field detector.

The $\text{BiFeO}_3\text{-NiFe}_2\text{O}_4$ and $\text{BiFeO}_3\text{-CoFe}_2\text{O}_4$ systems showed similar structural features. Therefore, only results for one of them are given in the following discussions. Figures

^{a)}Electronic mail: qzhan@berkeley.edu

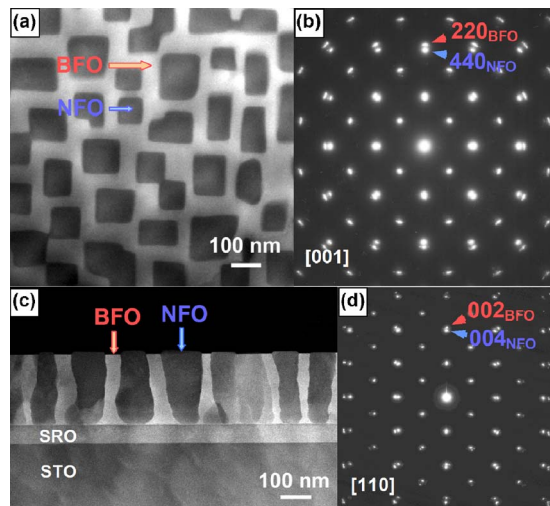


FIG. 1. (Color online) Low magnification Z-contrast images of the $\text{BiFeO}_3\text{-NiFe}_2\text{O}_4$ film and the corresponding diffraction patterns. [(a) and (b)] Plan view; [(c) and (d)] cross section.

1(a) and 1(c) give typical incoherent Z-contrast low magnification morphologies of the $\text{BiFeO}_3\text{-NiFe}_2\text{O}_4$ thin films from both plan-view and cross-section orientations and the corresponding electron diffraction patterns. Z-contrast imaging helps eliminate contrast contributions that originate from coherent strain effects and highlight mass-thickness differences. Thus it is especially suitable to investigate phase separation in composite films if the chemical composition of the phases is sufficiently different. In this experiment, BiFeO_3 containing heavy Bi atoms appears much brighter than phases that contain Ni or Co.

The magnetic NiFe_2O_4 pillars of about 100 nm of lateral dimension distribute homogeneously in the ferroelectric BiFeO_3 matrix and grew perpendicular to the substrate. The cross-section and plan-view single crystal diffraction patterns indicate that the films are not only epitaxial in the film normal direction but also in the film plane, giving a cube-on-cube orientation relationship $[001]_{\text{BFO}}//[001]_{\text{NFO}}$ and $(100)_{\text{BFO}}//(100)_{\text{NFO}}$. The interface between the two phases lies in the $\{110\}$ orientation.

A triple junction close to the substrate is shown in Fig. 2(a). Good wettability of BiFeO_3 on the SRO electrode was observed, which is expected because both of them have the perovskite structure. As manifested by the large contact angle, the spinel phase has poor wettability on the perovskite substrate, resulting in the tapering shape of the spinel pillars. Note that some NFO pillars did not grow directly on the

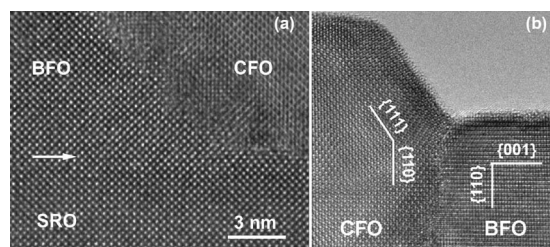


FIG. 2. (a) $\text{BiFeO}_3\text{-CoFe}_2\text{O}_4$ -substrate triple junction in the $[001]$ direction. The arrow indicates the film/substrate interface. (b) $\text{BiFeO}_3\text{-CoFe}_2\text{O}_4$ -substrate triple junction in the $[110]$ direction, showing the $\{001\}$ and $\{111\}$ facets of CoFe_2O_4 .

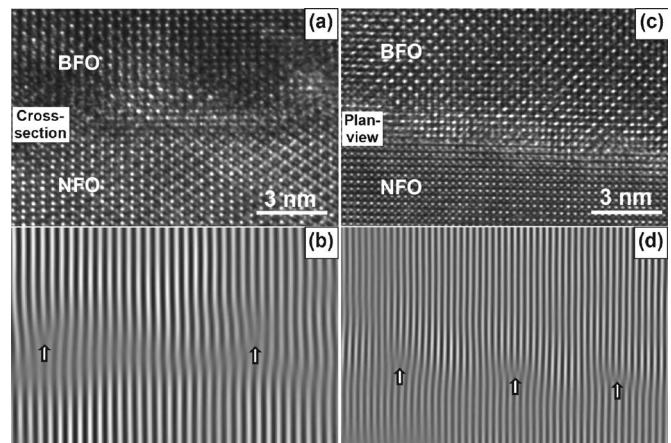


FIG. 3. High resolution images of the $\text{BiFeO}_3/\text{NiFe}_2\text{O}_4$ interface with the incident beam along (a) the $[110]$ cross-section orientation and (c) the $[001]$ plan-view orientation. (b) and (d) are the corresponding Fourier filtered images, revealing lattice mismatch clearly.

substrate, as indicated by a thin BiFeO_3 layer between the pillars and the substrate.

The spinel pillars form facets at the film surface [Fig. 1(c)]. Figure 2(b) shows a high resolution image of a $\text{BiFeO}_3\text{-CoFe}_2\text{O}_4$ -surface triple junction viewed along the $[110]$ direction, with both the surface facets and the interface in an edge-on orientation. The formation of the facets of CoFe_2O_4 strongly points to the role of the anisotropic surface energies in this crystal system with the (111) surface presenting the lowest energy, which is the case for most spinel phases.¹¹

A critical question of relevance to the coupling between ferroelectricity and magnetism at the interface is this: What is the degree of coherency at this interface? Conversely, is the 5% lattice mismatch relaxed? The high resolution images of the $\text{BiFeO}_3/\text{NiFe}_2\text{O}_4$ interface are given in Figs. 3(a) and 3(c) for cross-section and plan-view orientations, respectively. In order to reveal the lattice mismatch, the images are Fourier filtered by keeping only the Fourier components parallel to the interfaces, as shown in Figs. 3(b) and 3(d). For both the cross-section and plan-view orientations, an extra plane of BiFeO_3 occurs about every 20 planes, corresponding to $\sim 5\%$ misfit. Therefore, the lattice mismatch is fully relaxed both in the film plane and normal to the film. It should be noted that, while the Fourier filtering technique used above is helpful for the measurement of geometrical mismatch, it does not provide quantitative description of the strain field near the interface, which is beyond the scope of the present letter.

To understand the coupling mechanism among ferroelectricity, magnetism, and elasticity across the interface between the component phases, the answer to the question as how the two phases bond at the interface is a critical first step. As shown in Fig. 1, the interfaces between BiFeO_3 and NiFe_2O_4 lie in the $\{110\}$ orientation. In this family of planes, BiFeO_3 is composed of alternate BiFeO and O_2 layers, while NiFe_2O_4 is composed of alternate $(\text{Fe})[\text{Ni},\text{Fe}]\text{O}_2$ and $[\text{Ni},\text{Fe}]\text{O}_2$ layers. By joining either layer of the two sides, four possible interfaces can be formed. Considering the charges, the interfaces $[\text{BiFeO}]^{4+}/[(\text{Fe})[\text{Ni},\text{Fe}]\text{O}_2]^{1.5+}$ and $[\text{O}_2]^{4-}/[[\text{Ni},\text{Fe}]\text{O}_2]^{1.5-}$, where the superscripts denote the charges, can be immediately ruled out since the bonding layers contain like charges that would repel each other.

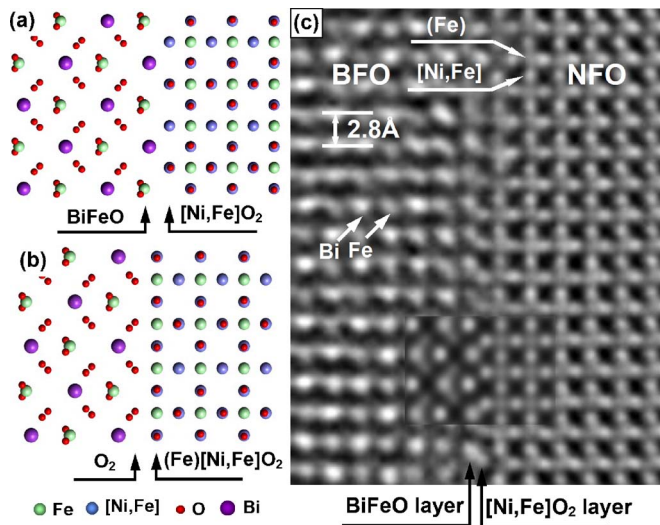


FIG. 4. (Color online) [(a) and (b)] Structure models of the BiFeO₃/NiFe₂O₄ interface; (c) phase of the electron exit wave in the [001] direction. The inset shows a simulated exit wave for model (a) at a thickness of 6 nm.

The remaining two configurations, written as $[\text{BiFeO}]^{4+}/[\text{[Ni,Fe]O}_2]^{1.5-}$ and $[\text{O}_2]^{4-}/[(\text{Fe})[\text{Ni,Fe]O}_2]^{1.5+}$, are shown in Figs. 4(a) and 4(b). From the charge point of view, both configurations are possible since the charge accumulation is suppressed to the same extent. Here we use the high resolution TEM to reveal the actual interface structure. Due to the objective lens aberrations, there is no apparent one-to-one correspondence between intensity extrema in conventional lattice images and the crystal structure projection. In order to obtain a direct projection of the crystal structure, the electron exit-wave reconstruction method (also called through focus series method)^{12–14} was used to investigate the interfaces at a truly atomic resolution. After reconstruction, the electron wave function at the exit plane of the object is free of imaging artifacts from the microscope and can exhibit a signal-to-noise ratio better than that of single input images. The phase of the complex electron exit wave, as shown in Fig. 4(c), was reconstructed from a series of 20 high resolution images of the BiFeO₃/NiFe₂O₄ interface with focus increments of 2.0 nm using the TRUEIMAGE software package.^{15,16}

Based on the one-to-one correspondence between atomic structure and exit wave, the complicated interface structure has been solved. It corresponds to the structure model illustrated in Fig. 4(a): BiFeO layer in BiFeO₃ matrix bonds to the [Ni,Fe]O₂ layer in NiFe₂O₄. A simulation of the exit-wave phase images using the structure model were also carried out, as shown in the inset in Fig. 4(c). Good agreement in terms of both the contrast and the atomic positions between the simulated and the experimental images was achieved.

The model shown in Fig. 4(b) was never observed experimentally. This can be rationalized by considering the structural continuity across the interface. As is well known for interfaces in crystalline materials,¹⁷ the perfect structural continuity is broken at interfaces and a rearrangement of chemical bonding occurs. Generally, the more the continuity across an interface, the less rearrangement is required, and

hence the lower the interface energy. For the interface we observed [Fig. 4(a)], it is the [Ni,Fe]O₂ layer in NiFe₂O₄ that bonds to BiFeO₃. Since both the [Ni,Fe]O₂ layer and BiFeO₃ have only octahedral sites, the structure continuity is maximized from the [Ni,Fe]O₂ layer to BiFeO₃. In contrast, the (Fe)[Ni,Fe]O₂ layer has tetrahedral sites, which cannot be accommodated in the perovskite structure, resulting in a larger rearrangement of bonding at the interface if (Fe)[Ni,Fe]O₂ bonded to BiFeO₃, and thus higher energy.

In summary, the structure and interface chemistry of composite thin films formed by BiFeO₃ and NiFe₂O₄/CoFe₂O₄ were studied at the nano and the atomic scales. Rectangular spinel nanopillars distribute homogeneously in the BiFeO₃ matrix, with the semicoherent interface lying in the {110} planes. The BiFeO layer in the BiFeO₃ matrix was found to bond to the [Ni,Fe]O₂ layer of the NiFe₂O₄ pillars, giving a minimized interface charging and a maximized structure continuity across the interface, which would result in strong elastic coupling.

This work has been supported by the ONR under a MURI program and a LBL-LDRD program. This material is based upon work supported by the National Science Foundation under Grant No. EEC-0425914. The authors acknowledge support of the National Center for Electron Microscopy, Lawrence Berkeley National Laboratory, which is supported by the U.S. Department of Energy under Contract No. DE-AC02-05CH11231.

¹V. Moshnyaga, B. Damaschke, O. Shapoval, A. Belenchuk, J. Faupel, O. I. Lebedev, J. Verbeeck, G. van Tendeloo, M. Mücksch, V. Tsurkan, R. Tidecks, and K. Samwer, *Nat. Mater.* **2**, 247 (2003).

²H. Zheng, J. Wang, S. E. Lofland, Z. Ma, L. Mohaddes-Ardabili, T. Zhao, L. Salamanca-Riba, S. R. Shinde, S. B. Ogale, F. Bai, D. Viehland, Y. Jia, D. G. Schlom, M. Wuttig, A. Roytburd, and R. Ramesh, *Science* **303**, 661 (2004).

³A. Artemev, J. Slutsker, and A. L. Roytburd, *Acta Mater.* **53**, 3425 (2005).

⁴F. Zavaliche, H. Zheng, L. Mohaddes-Ardabili, S. Y. Yang, Q. Zhan, P. Shafer, E. Reilly, R. Chopdekar, Y. Jia, P. Wright, D. G. Schlom, Y. Suzuki, and R. Ramesh, *Nano Lett.* **5**, 1793 (2005).

⁵H. Zheng, Q. Zhan, F. Zavaliche, M. Sherburne, F. Straub, M. P. Cruz, L. Q. Chen, U. Dahmen, and R. Ramesh, *Nano Lett.* **6**, 1401 (2006).

⁶G. Hu and Y. Suzuki, *Phys. Rev. Lett.* **89**, 276601 (2002).

⁷J. Wang, J. B. Neaton, H. Zheng, V. Nagarajan, S. B. Ogale, B. Liu, D. Viehland, V. Vaithyanathan, D. G. Schlom, U. V. Waghmare, N. A. Spaldin, K. M. Rabe, M. Wuttig, and R. Ramesh, *Science* **299**, 1719 (2003).

⁸F. Kubel and H. Schmid, *Acta Crystallogr., Sect. B: Struct. Sci.* **46**, 698 (1990).

⁹E. P. Wohlfarth, *Ferromagnetic Materials* (North-Holland, Amsterdam, 1982), Vol. 3, pp. 189.

¹⁰H. Zheng, J. Wang, L. Mohaddes-Ardabili, M. Wuttig, L. Salamanca-Riba, D. G. Schlom, and R. Ramesh, *Appl. Phys. Lett.* **85**, 2035 (2004).

¹¹R. K. Mishra and G. Thomas, *J. Appl. Phys.* **48**, 4576 (1977).

¹²C. L. Jia and A. Thust, *Phys. Rev. Lett.* **82**, 5052 (1999).

¹³R. R. Meyer, J. Sloan, R. E. Dunin-Borkowski, A. I. Kirkland, M. C. Novotny, S. R. Bailey, J. L. Hutchison, and M. L. H. Green, *Science* **289**, 1324 (2000).

¹⁴C. Kisielowski, C. J. D. Hetherington, Y. C. Wang, R. Kilaas, M. A. O'Keefe, and A. Thust, *Ultramicroscopy* **89**, 243 (2001).

¹⁵W. M. J. Coene, A. Thust, M. Op de Beeck, and D. Van Dyck, *Ultramicroscopy* **64**, 109 (1996).

¹⁶A. Thust, W. M. J. Coene, M. Op de Beeck, and D. Van Dyck, *Ultramicroscopy* **64**, 211 (1996).

¹⁷A. P. Sutton and R. W. Balluffi, *Interfaces in Crystalline Materials* (Clarendon, Oxford, 1995), pp. 240.